

1 Immunity and bacterial recruitment in plant leaves are parallel 2 processes whose link shapes sensitivity to temperature stress

3 Jisna Jose^{1,9}, Erik Teutloff¹, Simrat Naseem¹, Emanuel Barth^{2,4}, Rayko Halitschke^{3,9}, Manja
4 Marz^{2,5,6,7,8,9}, and Matthew T. Agler^{1,9*}

5 ¹ Institute for Microbiology, Plant Microbiosis Group, Friedrich Schiller University Jena, Neugasse 23,
6 Jena 07743, Germany.

7 ² RNA Bioinformatics and High-throughput analysis, Faculty of Mathematics and Computer Science,
8 Friedrich Schiller University Jena, Jena, Germany.

9 ³ Department of Biochemistry, Max-Planck Institute for Chemical Ecology, Hans-Knöll-Straße 8, Jena
10 07745, Germany.

11 ⁴ Bioinformatics Core Facility Jena, Friedrich Schiller University Jena, Leutrgraben 1, 07743 Jena,
12 Germany

13 ⁵ Leibniz Institute for Age Research, FLI, Beutenbergstraße 11, Jena 07743, Germany

14 ⁶ European Virus Bioinformatics Center, Friedrich Schiller University, Leutrgraben 1, Jena 07743,
15 Germany

16 ⁷ German Center for Integrative Biodiversity Research (iDiv), Puschstraße 4, Leipzig 04103, Germany

17 ⁸ Michael Stifel Center Jena, Friedrich Schiller University, Ernst-Abbe-Platz 2, Jena 07743, Germany

18

19 ⁹ Cluster of Excellence Balance of the Microverse, Friedrich Schiller University, Furstengraben 1, Jena
20 07743, Germany

21

22 *Corresponding author:

23 Matthew T. Agler

24 The Plant Microbiosis Lab, Institute of Microbiology

25 Friedrich Schiller University Jena

26 Neugasse 23

27 07743 Jena, Germany

28 E-mail: matthew.agler@uni-jena.de

29 Tel: +49 (0)3641 9 49980

30

31 Abstract

32 Rising global temperatures necessitate developing climate-resilient crops with better adaptability to
33 changing climates. Under elevated temperatures, plant immunity is downregulated, putting them at risk
34 of foliar pathogen attack. Manipulating plant defense hormones is one way to mitigate this detrimental
35 effect. However, it is unclear how plant immunity interacts with plant microbiome assembly and how
36 temperature will thus affect overall plant health and stability. We used chemical mutagenesis to identify
37 a phenotypically healthy genotype of *A. thaliana*, “CLLF”, that compared to the wild type naturally
38 recruits an altered leaf bacteriome, including unusually high bacteria loads. Simultaneously, CLLF
39 hyperaccumulates salicylic acid (SA) and jasmonates, has constitutively upregulated systemic and
40 innate defenses, and has increased resistance to necrotrophic fungal and hemi-biotrophic bacterial
41 pathogens, indicating that pathogen immunity and non-pathogen recruitment function in parallel.
42 Growth of specific non-pathogenic leaf bacteria on SA as a carbon source suggests the same hormones
43 may even link the two processes. CLLF also showed high tolerance to heat stress in comparison to the
44 wild type, but SA-associated defense processes are not downregulated under heat. Synthetic community
45 (SynCom) experiments showed that when the taxonomic diversity of bacteria available to CLLF is
46 artificially reduced, resilience to heat stress is compromised, leading to dysbiosis, but this does not
47 occur with the full SynCom or in the wild type with any SynCom. Thus, the downregulation of defenses
48 in response to heat may contribute to avoidance of dysbiosis caused by some leaf bacteria, but full
49 bacteriome taxonomic diversity can restore balance.

50 Significance Statement

51 Plants are living ecosystems colonized by diverse microorganisms who strongly shape host health.
52 Understanding how balance arises in host-associated microbiomes is a key step to understanding how
53 to preserve, manage and possibly optimize these complex ecosystems, especially in a changing climate.
54 Using a random mutagenesis approach in a natural *A. thaliana* ecotype, we find that constitutively
55 upregulated defenses are associated with both tolerance to (a)biotic threats and healthy recruitment of
56 leaf bacteria, very likely in a direct manner. Thus, immunity and bacterial recruitment in leaves operate
57 in parallel. Synthetic community experiments show further that this link plays important roles in
58 shaping plant resilience to heat stress, an important consideration in developing plants more stable to
59 climate change.

60

61 Introduction

62 Extreme conditions such as high temperature, drought, salinity, and high humidity due to climate
63 change may adversely affect agriculture and crop productivity. One reason is that changes in ambient
64 growth conditions that affect plant physiology and development, in turn, can alter plant-microbe
65 interactions, an inter-dependence known as the “disease triangle” (1). Altered plant-microbe
66 interactions carry the risk that balance in the microbiome may be lost, leading to dysbiosis, including
67 devastating plant diseases and loss of productivity. Thus, it is important to understand how plants
68 establish and maintain balance in the microbiome and how environmental factors will affect that
69 balance.

70 Leaf-colonizing bacteria are an important component of the microbiome with regard to plant health
71 because they protect plants but also must be regulated to prevent disease (2). Plants use a variety of
72 mechanisms to recruit bacteria and maintain balance. The phyllosphere (leaf) bacteriome is assembled
73 from both soil-born and air-born inoculums in either a deterministic or stochastic manner (3, 4). Plant
74 defenses, besides establishing immunity to pathogens, also plays critical roles in maintaining balance
75 in the bacteriome. For one, the interaction of commensal and opportunistic pathogenic bacteria with
76 immune components like MAMP-triggered immunity helps prevent dysbiosis by preventing
77 overgrowth of opportunistic pathogens (5–7). Additionally, secondary metabolites can contribute to
78 assembly via their toxicity (8) and likely by serving as resources for bacteria particularly adapted to use
79 them (9, 10). However, how plant immunity against (opportunistic) pathogens is more broadly linked
80 to the parallel process of bacteriome assembly in healthy leaves remains unclear.

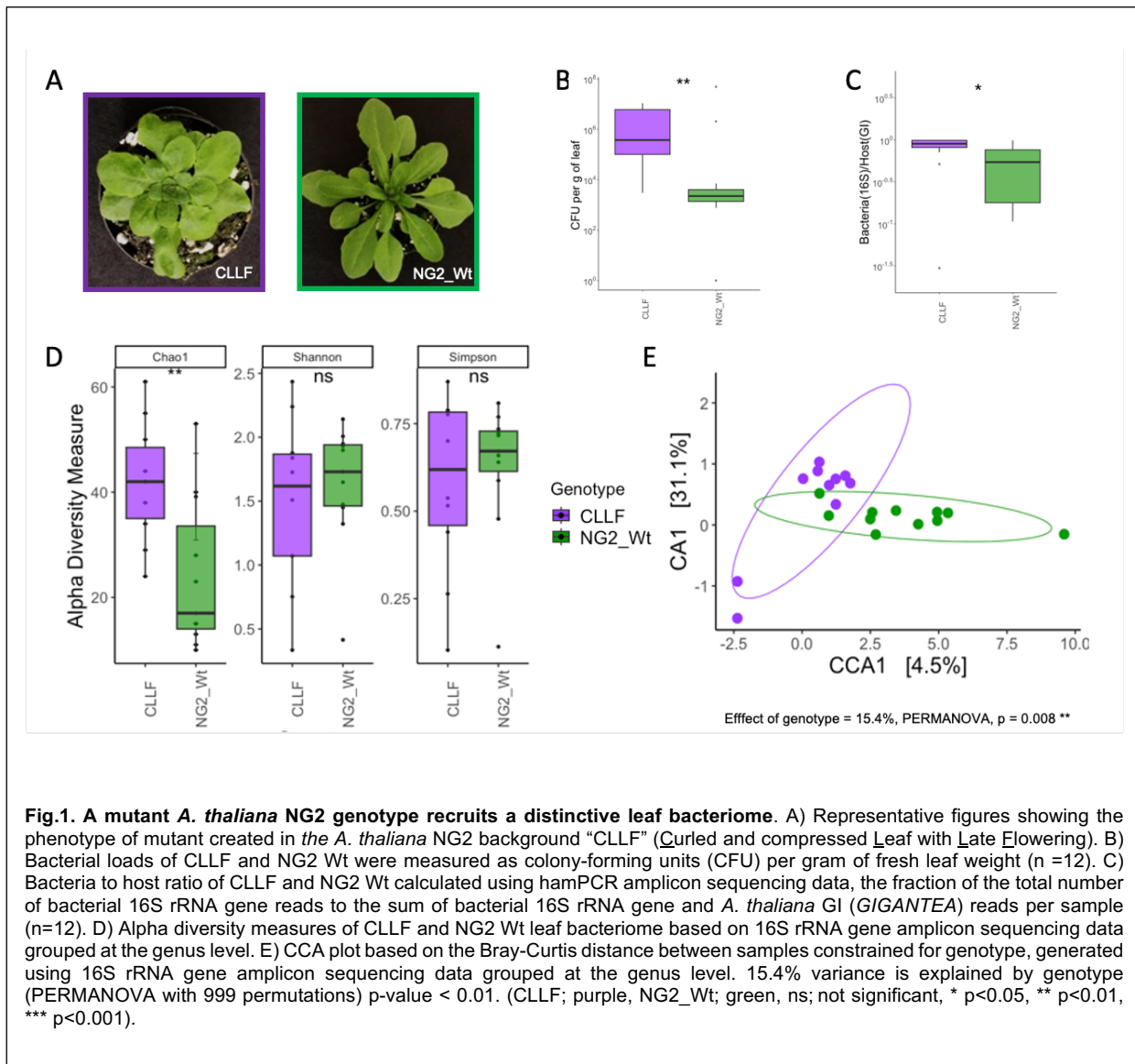
81 The plant immune system is itself affected by the abiotic environment. Although the mechanisms
82 linking abiotic stressors to plant immunity are still underexplored, the effect of temperature is perhaps
83 best studied. For example, at moderately high temperatures (30°C vs. 23°C), the production of salicylic
84 acid (SA), a major plant defense hormone, is suppressed (11). Jasmonic acid (JA) biosynthesis is also
85 involved in temperature-dependent susceptibility of rice blast disease (12). Abscisic acid (ABA)
86 biosynthesis was not affected by heat stress, but ABA does negatively affect R gene-mediated immune
87 responses at high temperatures (13). Because of compromised immunity, these changes lead to
88 increased susceptibility to pathogens. Some microbes help plants mitigate heat stress by making them
89 more resilient (14, 15), suggesting that the leaf microbiome could offset some adverse effects of
90 increased temperature.

91 We hypothesized that the balance established by plant immune components during the natural
92 recruitment of leaf bacteriomes plays important roles in resilience to temperature stress. To investigate
93 these questions, we first studied how plant physiology shapes balance in the leaf bacteriome of a wild
94 *A. thaliana* genotype by generating a random mutant genotype that is healthy, but which naturally
95 assembles an alternatively balanced leaf bacteriome. We then studied immune signaling in the mutant

96 and responses to pathogens and temperature stress. Finally, we tested how the balanced bacteriome
97 compensates for altered immune responses to temperature.
98

99 **Results**

100 *A phenotypically distinct mutant displays an altered leaf bacteriome*

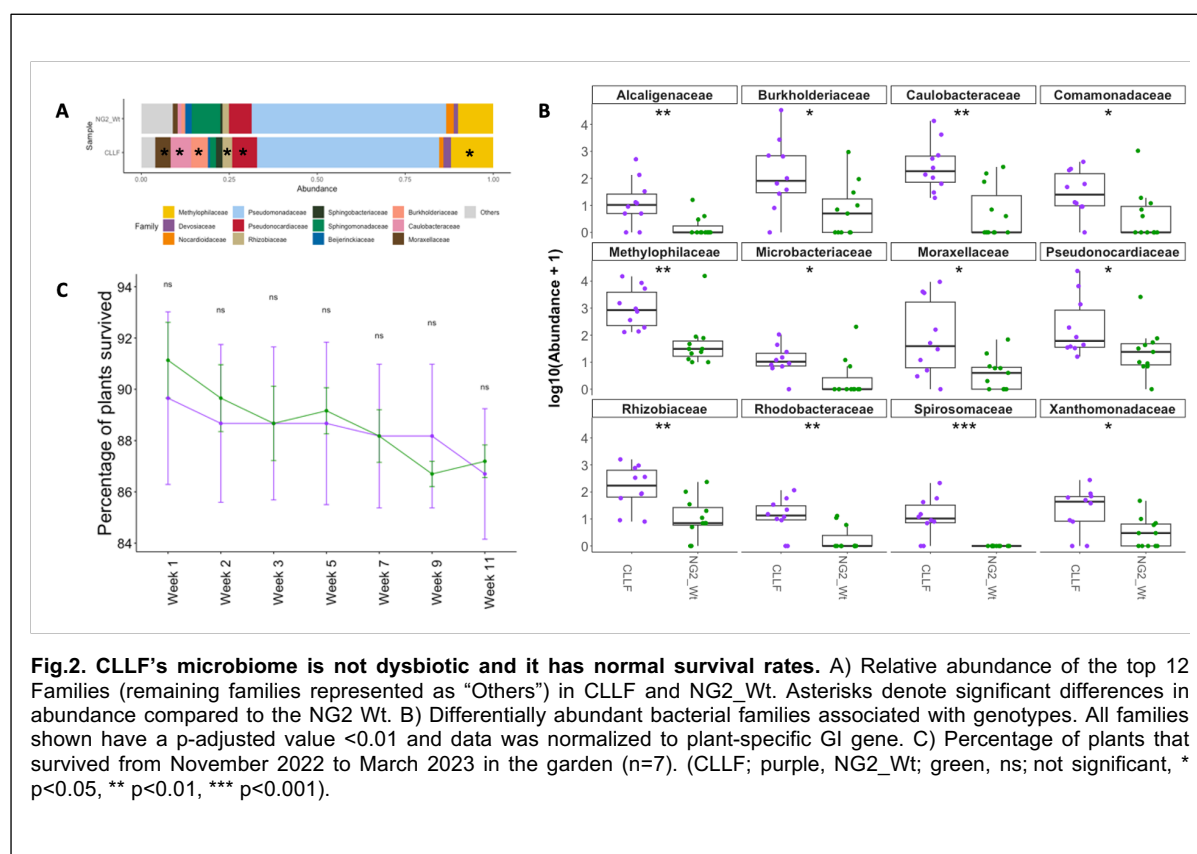


101 We previously established a collection of *Arabidopsis thaliana* ecotypes collected from Jena, Germany
 102 (16). For this study, we generated a mutant plant library in ecotype NG2 using chemical mutagenesis
 103 (see methods). In the M2 generation, we screened hundreds of mutant plants for higher bacterial load
 104 than the wild type (WT). Approximately 5% of the mutant population had a higher bacterial load
 105 (although this was only based on n=1 because every seed is a unique genotype), indicating altered
 106 microbiota recruitment (Supplementary Fig.1). The mutant used further in this study, “CLLF”, had the
 107 highest bacterial load. In addition to that, it had a distinct phenotype, curled, and compressed leaves
 108 with late flowering compared to the wild type (Fig 1A).

109 Whole leaf bacteriomes were characterized in the NG2 wild type (NG2 Wt), and the M4 generation of
 110 CLLF (which should be mostly homozygous) grown in commercial soil supplemented with an extract
 111 of natural soil. A plastic barrier was used to separate rosettes from soil (see methods) to ensure that

112 colonization differences were not due to increased CLLF leaf-soil direct contact. In 3-week-old plants,
 113 bacterial loads in leaves of CLLF (colony-forming units) were approximately 100-fold higher compared
 114 to the wild type. We also confirmed higher loads using the sensitive hamPCR method (17) (Fig.1B and
 115 1C, $p < 0.01$ and $p < 0.05$, respectively). In addition, CLLF leaves recruited more diverse bacterial genera
 116 than the wild type (Fig.1D, Chao1 $p < 0.01$) with a similar evenness (Fig. 1D, Shannon, and Simpson
 117 indices). Furthermore, CLLF leaf bacteriome samples were more densely clustered and were separated
 118 from NG2 wildtype in canonical correspondence analysis (CCA) of the Bray-Curtis distances between
 119 samples (Fig.1E, 15.4% variation explained by the genotype, PERMANOVA, $p = 0.008$, 999
 120 permutations). The distinct beta diversity patterns, higher alpha diversity, and high bacterial loads
 121 together confirm an altered leaf microbiota recruitment in CLLF. Similar results were found without
 122 the plastic barrier in three independent experiments (Supplemental Fig.2).

123 *CLLF's altered recruitment is not dysbiotic*



124 To check whether the healthy CLLF phenotype indicated a more taxonomically balanced bacteriome
 125 than previously described "dysbiotic" mutants (over-colonization by one or a few opportunistic
 126 pathogens), we looked closer at the taxonomic composition of the CLLF leaf bacteriome. Overall,
 127 CLLF recruited similar bacterial families as the wild type (Fig. 2A). However, multiple families were
 128 significantly more abundant in CLLF (p -value ≤ 0.01) (Fig. 2B). Differentially abundant taxa that were
 129 significantly correlated to the genotype included members of most leaf-colonizing phyla. One-third of

130 the differentially abundant taxa were Betaproteobacteria (order Burkholderiales, families
131 Alcaligenaceae, Burkholderiaceae, Comamonadaceae, and Methylophilaceae), one-fourth of the
132 differentially abundant taxa were Alphaproteobacteria (Caulobacteraceae, Rhizobiaceae, and
133 Rhodobacteraceae), two families each belonging to Actinomycetota (Microbacteriaceae and
134 Pseudonocardiaceae) and Gammaproteobacteria (Moraxellaceae and Xathomonadaceae) and one
135 family belonging to Bacteroides (Spirosomaceae). Thus, the higher bacterial load of CLLF is not due
136 to the enrichment of a single or a few taxa, which should lead to dysbiosis, but rather an apparently
137 balanced enrichment of multiple families.

138 In support of balance in the CLLF bacteriome, plants were never observed to develop a disease
139 phenotype in the lab (Fig.1A). To test this further, we assessed CLLF's survival during overwintering
140 in nature in an outdoor garden experiment. CLLF had a similar survival rate as wild-type NG2 plants
141 (Fig.2C). Furthermore, leaf functions of CLLF were only slightly altered compared to wild type.
142 Specifically, the electron transport rate (ETR) and the vapor pressure differential were slightly higher,
143 and the stomatal conductance was slightly lower in CLLF compared to the wild type (p -value < 0.01)
144 (Supplementary Fig. 3). Together, these results suggest that the mutant phenotype of CLLF leads to the
145 recruitment of an alternate, but balanced, bacteriome.

146 *CLLF's immune system is intact and constitutively active*

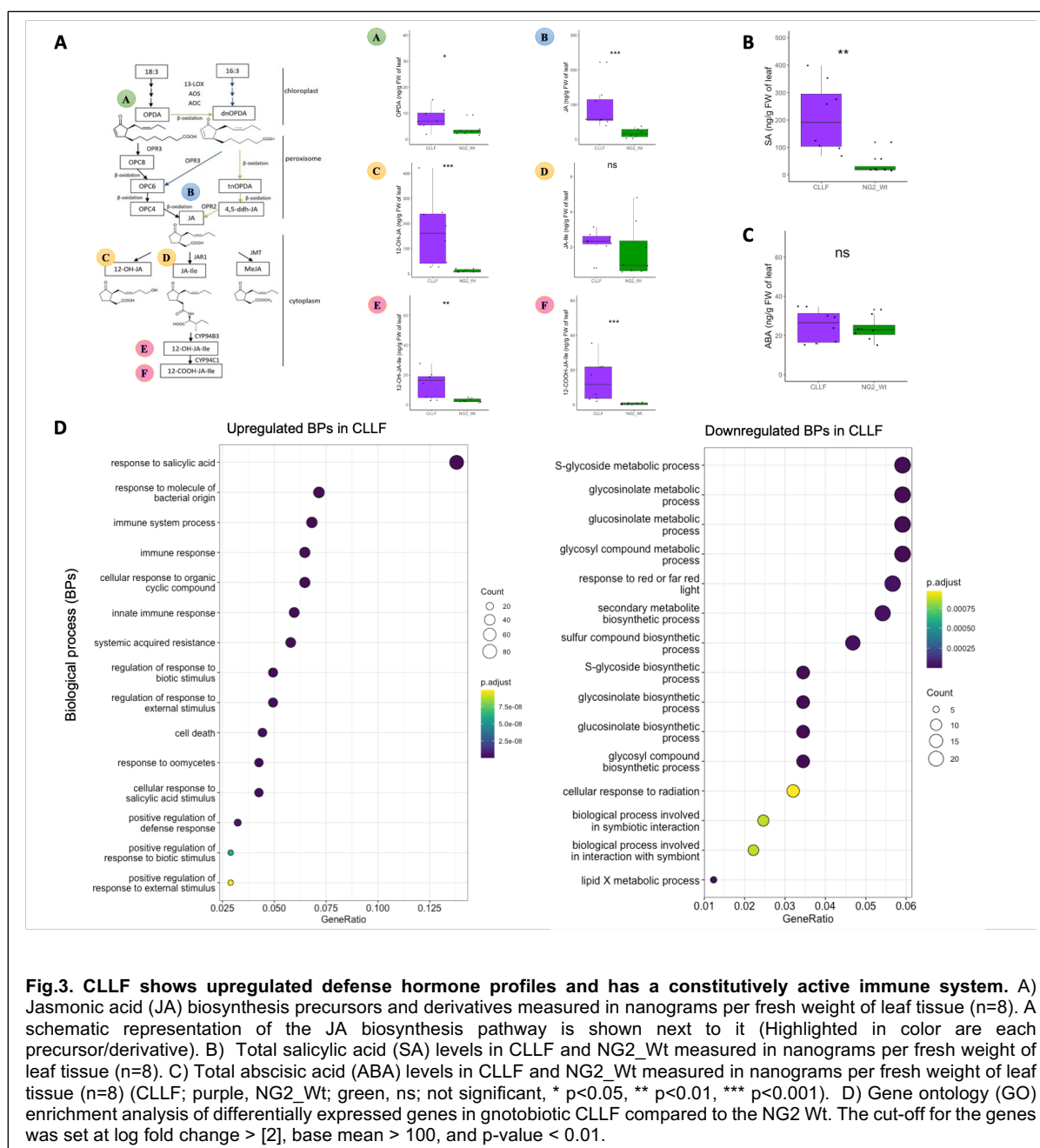
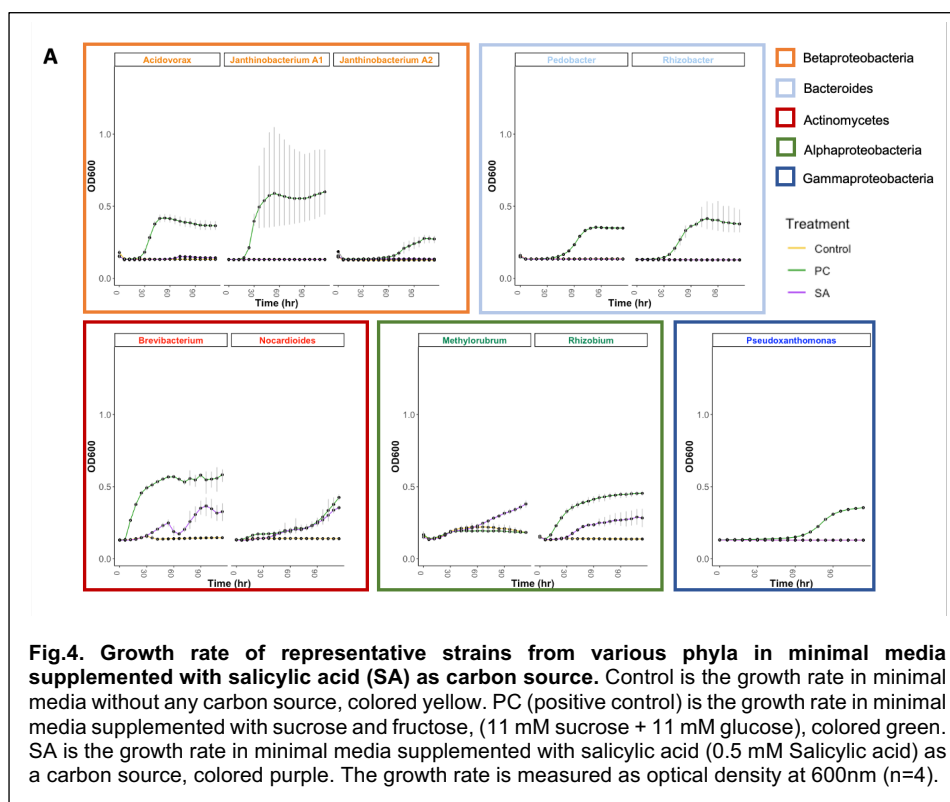


Fig.3. CLLF shows upregulated defense hormone profiles and has a constitutively active immune system. A) Jasmonic acid (JA) biosynthesis precursors and derivatives measured in nanograms per fresh weight of leaf tissue (n=8). A schematic representation of the JA biosynthesis pathway is shown next to it (Highlighted in color are each precursor/derivative). B) Total salicylic acid (SA) levels in CLLF and NG2_Wt measured in nanograms per fresh weight of leaf tissue (n=8). C) Total abscisic acid (ABA) levels in CLLF and NG2_Wt measured in nanograms per fresh weight of leaf tissue (n=8) (CLLF; purple, NG2_Wt; green, ns; not significant, * p<0.05, ** p<0.01, *** p<0.001). D) Gene ontology (GO) enrichment analysis of differentially expressed genes in gnotobiotic CLLF compared to the NG2 Wt. The cut-off for the genes was set at log fold change > [2], base mean > 100, and p-value < 0.01.

147 To test whether the CLLF immune system is intact, we investigated defense hormone levels. Notably,
 148 CLLF exhibited constitutively higher levels of defense hormones, with upregulated salicylic acid (SA)
 149 (Fig.3B) and jasmonates (Fig.3A). CLLF plants grown in axenic conditions also showed higher levels
 150 of SA and jasmonates (Supplementary Fig.4), indicating that the constitutive production of these
 151 hormones is microbe-independent.

152 Next, we analyzed CLLF gene expression relative to NG2 Wt plants. In agreement with the
 153 overproduction of defense hormones, gene expression profiles underscored CLLF's constitutively
 154 active immune system. Genes involved in response to SA, systemic acquired resistance (SAR),

155 responses to bacterial molecules, and oomycetes were among the highest upregulated in CLLF (Fig.3D).
156 The strongest downregulated genes were mostly involved in glucosinolate-related processes.
157 We reasoned that an overactive immune system may still be dysfunctional, which could explain the
158 higher commensal bacterial loads. However, CLLF plants were more resistant to the bacterial pathogen
159 *Pseudomonas syringae* pv. *syringae* DC3000 (Supplementary Fig. 5C) and showed higher resilience
160 towards the fungal pathogen *Sclerotinia sclerotiorum* (Supplementary Fig. 5A and 5B) than the wild
161 type. Thus, CLLF appears able to mount a functional immune response. Therefore, the role of plant
162 defenses in maintaining plant immunity works in parallel with the recruitment of non-pathogenic leaf
163 bacterial communities.
164 *Some leaf bacteria may directly utilize hormones as a resource for growth*



165 High SA levels were previously linked to increased bacterial diversity in the phyllosphere (18), and SA
166 has been suggested to recruit specific taxa directly in the rhizosphere (9). Thus, we hypothesized that
167 plant hormones may simultaneously shape plant immunity and recruit leaf bacteriomes, explaining the
168 seemingly counterintuitive resistance and recruitment phenotypes of CLLF. To test this, we checked
169 whether strains representative of diverse CLLF phyla could utilize salicylic acid as a carbon source (Fig
170 4). We found that some bacteria belonging to Alphaproteobacteria (Rhizobium and Methyloburum)
171 and Actinomycetes (Nocardioideis and Brevibacterium) showed growth in minimal media supplemented
172 with 0.5mM salicylic acid. However, the Burkholderiales and Bacteroides we tested did not show
173 growth in SA *in vitro*. Thus, overproduction of SA and possibly other hormones in the phyllosphere at

174 least have the potential to contribute directly to the recruitment of specific bacterial taxa that can
175 metabolize them, as previously suggested.

176 *High defense-related gene expression in CLLF does not decrease at elevated temperatures*

177 A well-known effect of moderately high temperatures in plants is decreased expression of defense-
178 related genes, which causes increased pathogen susceptibility. During an accidental breakdown of plant
179 growth chambers in which temperatures of 34°C were reached, we observed that CLLF showed higher
180 tolerance to the extreme temperature than the wild type (Supplementary Fig. 5D), which could be caused
181 by increased SA signaling (19). To better understand this, we looked at what genes were differentially
182 regulated in CLLF with and without a controlled high temperature (30°C) treatment relative to NG2 Wt
183 plants (Supplementary Fig. 6). Overall, the gene expression profile of CLLF did not strongly change
184 due to heat treatment (Supplementary Fig. 6A). Specifically, very few genes and associated biological
185 processes were up- or down-regulated only in response heat treatment (Supplementary Fig. 6B). In
186 contrast, almost all processes differentially regulated in CLLF relative to NG2 Wt in normal conditions
187 were similarly regulated after heat treatment (Supplementary Fig. 6C). This included immune
188 activation-related processes, although a downregulation would typically be expected at elevated
189 temperatures (11). Thus, the constitutively active immune system of CLLF also does not suffer from
190 down-regulation of immune signaling in response to high temperature.

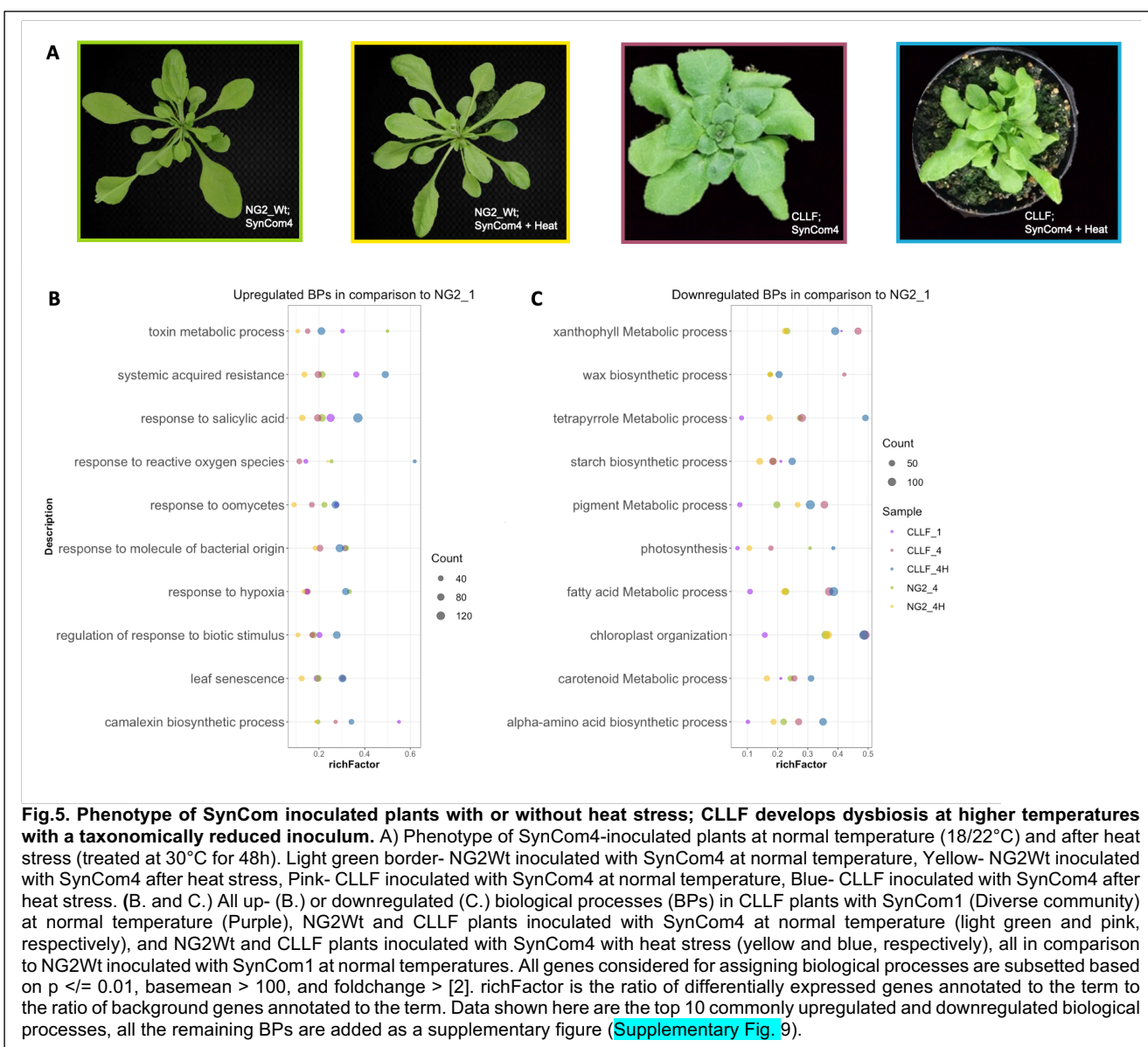
191 *The balanced CLLF bacteriome is required to prevent dysbiosis at high temperatures*

192 Because CLLF's activated immune system was linked to the alternative bacteriome balance and
193 downregulation of immune responses at high temperatures was inactive in CLLF, we decided to
194 investigate the role of bacteriome composition on balance during temperature stress. Therefore, we
195 used a semi-ghnotobiotic synthetic community (SynCom) experiment (see methods). Plants were pre-
196 inoculated with either a full SynCom representative of the entire CLLF bacteriome (SynCom1) or
197 SynComs that lacked major taxonomic groups. This setup allowed us to evaluate whether significant
198 losses in taxonomic diversity would affect balance. SynCom2 lacked Burkholderiales
199 (Comamonadaceae and Oxalobacteriaceae), SynCom3 lacked Bacteroidota (Flavobacteriaceae and
200 Sphingobacteriaceae), and SynCom4 lacked both groups (Supplementary Fig 7 and Supplementary
201 Table 1). Notably, the bacteria remaining in SynCom4 include Actinomycetes and Alphaproteobacteria
202 that can utilize salicylic acid as a carbon source (Fig 4).

203 Plants not exposed to heat displayed normal, healthy phenotypes with all SynComs (Fig 5A and
204 Supplementary Fig. 8A). We next evaluated gene expression profiles of NG2 Wt and CLLF treated
205 with SynCom1 and the reduced SynCom4. As expected, compared to NG2 Wt with SynCom1, CLLF
206 with SynCom1 showed upregulation of various immune responses (Fig 5B), similar to the response
207 after growth in normal soil (Fig 3D). In response to SynCom4, NG2 Wt showed significantly increased

208 immune responses, phytoalexin biosynthetic pathways, and decreased photosynthesis-related genes,
209 while CLLF maintained high defense-related gene expression (Fig 5B and 5C). Thus, removing
210 Burkholderiales and Bacteroides in SynCom4 appeared to result in a disbalance that NG2 Wt addressed
211 with a defense response. CLLF was likely able to maintain balance due to already upregulated immune
212 responses.

213 Upon exposure to 30°C for 48-h, NG2 Wt plants showed a normal, healthy phenotype regardless of the
214 SynCom (Fig 5 and Supplementary Fig. 8B). Immune system-related biological processes that were
215 upregulated in NG2 Wt plants with SynCom4 under normal conditions decreased expression following
216 heat treatment. Thus, the NG2 Wt regulated immune genes as previously described due to heat, and this
217 appears to have been the appropriate response even with a highly reduced bacterial community, since
218 the plants remained healthy. In CLLF with SynCom4, on the other hand, we observed a strong effect of
219 heat stress (Fig. 5A and Supplementary Fig. 8C). Symptoms included deformed rosettes and chlorosis.
220 In these plants, immune responses, genes related to senescence, and low oxygen were extremely highly
221 upregulated, suggesting a potential growth-defense tradeoff. CLLF with SynCom1, on the other hand,
222 showed no signs of a dysbiotic phenotype under heat treatment (Supplementary Fig.8 and 9). Together,
223 these results suggest that with an incomplete bacteriome, proper immune system regulation in response
224 to temperature helps avoid dysbiosis. However, a complete bacteriome counteracted dysbiosis,
225 suggesting that leaf microbiome diversity can strongly contribute to host stability under abiotic stress
226 and contribute resilience to overcome altered immune signaling regulation. Notably, CLLF always
227 showed higher resistance than NG2 Wt to *Pseudomonas syringae* pv. *syringae* DC3000 (Pst DC3000),
228 even when inoculated with SynCom4 and after heat treatment (Supplementary Fig. 10). This further
229 supports that the mechanism of the observed growth-defense imbalance under temperature is linked to
230 microbiome assembly and is distinct and functions in parallel to the mechanisms of pathogen resistance.



232 Discussion

233 The absence of key components of the immune system was previously shown to lead to dysbiosis - a
234 breakdown of a healthy plant microbiome (5, 7). In these cases, disease phenotypes were characterized
235 by high growth of specific taxa, suggesting that plant immune systems maintain balance by preventing
236 the proliferation of opportunistic pathogens (2). Here, we identified CLLF, a mutant genotype with
237 unusually high leaf bacterial loads when grown in natural soil. Detailed phenotyping revealed that the
238 mutant has a constitutively active and apparently fully functional immune system despite high loads.
239 Compared to the previously reported dysbiotic bacteriomes in immune-deficient mutants (5, 7), CLLF
240 was healthy, robust, had a high abundance of diverse leaf-associated bacterial taxa, and no overgrowth
241 of specific opportunistic pathogenic taxa. Thus, the constitutively active immune system of CLLF and
242 associated high bacterial loads appear to represent an alternative balanced state of the leaf bacteriome.
243 This finding suggests that although high bacterial loads indicate disease when opportunistic pathogens
244 proliferate (20), balanced recruitment can stabilize higher loads. The findings also show that increased
245 recruitment of non-pathogenic bacteria is compatible with and may even be directly linked to a fully
246 functional and active immune system.

247 The observation that constitutively activated immunity was strongly correlated to leaf bacterial
248 recruitment in CLLF could partly be explained by the ability of bacteria to use plant defense signals
249 directly as resources for growth. It is already well-known that some bacteria can grow on SA directly
250 (21) and SA was previously suggested to play positive direct roles in rhizosphere recruitment (9) and
251 in promoting leaf bacterial diversity (18). SA is also likely available to leaf colonizers since it
252 accumulates in extracellular compartments (e.g., apoplast) upon activation of immunity (22). In our
253 tests, the growth of bacterial taxa used in the SynCom experiments on SA followed taxonomic
254 boundaries: None of the Burkholderiales or Bacteroides tested showed growth in SA, while the tested
255 alphaproteobacteria and actinobacteria did (SA consumers). Thus, a role for SA in the recruitment of
256 these taxa is plausible.

257 Apart from SA, the CLLF mutant also accumulated jasmonates, including OPDA and JA, relative to
258 NG2 Wt. Although this did not include the best-studied active form, JA-isoleucine, molecules such as
259 OPDA play important roles in defense, thermotolerance, and regulation of other plant hormones (23,
260 24). JA species have also been shown to have effects on activity of specific plant-associated bacteria,
261 including functioning as a chemoattractant and inducing the formation of biofilms in the rhizosphere
262 (25, 26). Additionally, the aliphatic glucosinolate profile of CLLF was significantly altered compared
263 to the wild type (data not shown here). Some bacteria can metabolize glucosinolates, and accordingly,
264 we previously found that leaf glucosinolates function in bacterial recruitment, likely by acting as a
265 carbon source for specific taxa (10, 27). This recruitment depends on the glucosinolate species, so the
266 changed glucosinolate chemotype in CLLF likely also contributed to the altered leaf microbiome. Thus,

267 we hypothesize that the secondary metabolites linked to the plant immune system also function in direct
268 and specific recruitment processes for non-pathogenic leaf bacteria.

269 Alternative roles of plant hormones are not surprising since they are ancient signals in the green lineage
270 and, therefore, likely serve various purposes. SA-responsive NPR proteins, for example, appear to be
271 SA receptors in all plants, but conserved ancient functions shared by both bryophytes and tracheophytes
272 include light and temperature sensing, but not defense which probably evolved later (28). At any rate,
273 if defense signals help recruit leaf bacteria, forward genetics approaches such as mutant screens used in
274 this study could be a promising way to engineer plant microbiomes in a targeted way by screening for
275 changes in specific metabolites. However, to leverage such an approach, further research is needed to
276 determine how specific metabolites function in different contexts to recruit bacteria and how
277 microbiome balance is impacted by resource utilization.

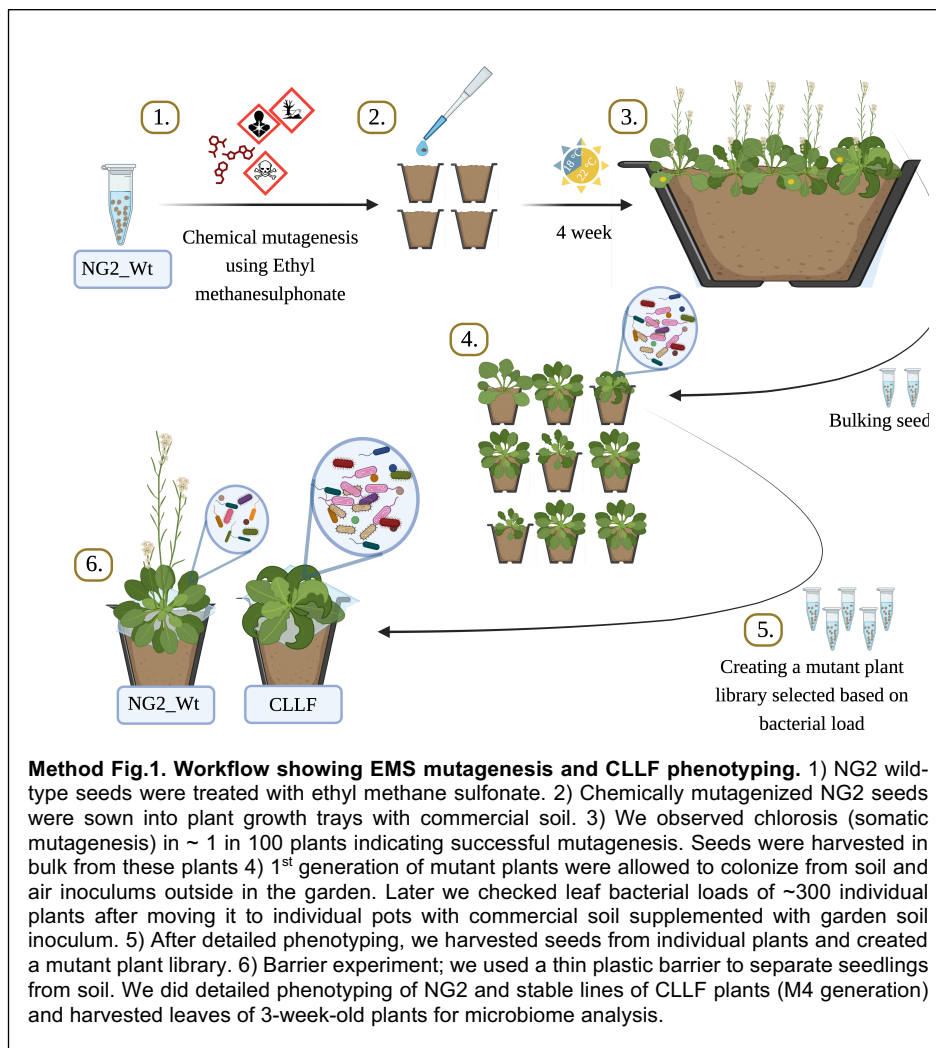
278 The salicylic acid (SA) pathway is integral to plant resistance and immunity, playing major roles in
279 abiotic and biotic stress tolerance (28, 29). Down-regulation of SA biosynthesis at high temperatures
280 makes plants prone to infection by plant pathogens (29). Thus, both exogenous SA applications and
281 manipulating immune regulation to increase SA accumulation under higher temperatures have been
282 suggested as remedies (19, 30). However, it is unclear how altering the regulation of immunity at higher
283 temperatures will affect plant interactions with the broader microbiome. Here, the mutant CLLF
284 genotype showed many expected signs of constitutive and heat-insensitive SA-dependent immune
285 upregulation: Higher tolerance to plant pathogens under both conditions and higher tolerance to heat
286 stress than the wild-type. While this did not cause problems at normal temperatures, plants exposed to
287 a reduced microbiota showed extreme dysbiosis at higher temperatures. One explanation could be that
288 the upregulation of SA signalling under heat stress may have fuelled the overgrowth of SA consumers
289 that were not balanced by other colonizers, resulting in a growth-defense imbalance. Accordingly,
290 CLLF plants pre-inoculated with a fully diverse bacteriome did not show dysbiosis, indicating that a
291 full bacteriome diversity contributes resilience to altered immune signaling regulation.

292 In conclusion, our results suggest that alternative states of balance exist in the phyllosphere microbiome.
293 Specifically, plant immune activation alters the balance in the phyllosphere microbiome by altering
294 recruitment patterns without necessarily creating dysbiosis. We hypothesize that this occurs because
295 plant defense hormones, besides acting as defense signals, are also plant-bacterial communication
296 signals, driving colonization of the non-pathogenic bacteriome. However, as we observed, this implies
297 that hormone balance will play key roles in maintaining a stable microbiome under environmental
298 stressors. The microbiome of plants colonized in nature depends on both the environment and chance
299 colonization events (31), so not all taxa are always present. Given this risk, plants may have evolved to
300 prevent upregulation of defense signals under heat stress, at least in part, to mitigate the possibility of
301 imbalance caused by the proliferation of taxa that grow in response to defense signals. Thus, as
302 manipulating plants to better deal with multiple stressors increasingly finds use to combat changing
303 climates (32), it is important to consider how altered signaling patterns will affect interactions with the

304 diversity of the plant-associated bacteriome. In particular, strategies to ensure a full diversity is available
305 for colonization may help avoid unintended consequences.
306

307 Materials and Methods

308 *EMS mutagenesis*



309 A well-characterized *Arabidopsis thaliana* ecotype “NG2” (NASC ID N2110865; Je-1) previously
310 collected from Jena, Germany was used for this study (16). Approximately 5000 seeds of *A. thaliana*
311 NG2 seeds were incubated with 0.3% ethyl methane sulphonate (EMS, Sigma-Aldrich; M0880-1G)
312 overnight as previously described (33). After repeated washing with sterile Milli-Q water, the M1 seeds
313 were resuspended in 0.1% agarose. Seeds were vernalized for 5 days at 4°C and sowed into soil (2:1
314 Floraton 3 Floragard Potting soil and perlite supplemented with 25g/ 6L soil mix substral osmocote as
315 fertilizer) as batches of 100 plants per tray and moved to a growth cabinet set at 22°C day-16h/18°C
316 night- 8h cycle. Chlorotic spots were observed in roughly one in a hundred plants after 2.5 weeks,
317 indicating somatic mutagenesis. Once the plants started producing seeds, siliques were harvested in
318 bulk from each tray. Later, approximately 200 seeds collected from each tray were sown into a natural
319 garden soil after surface sterilization and vernalization. Two weeks after germination, approximately
320 300 healthy M2 seedlings were randomly selected and transferred into individual pots containing
321 commercial soil supplemented with garden soil inoculum (60g natural garden soil dissolved in 1L

322 autoclaved Milli-Q water, mixed with 3L commercial soil) and moved to growth shelves. The plants
323 were allowed to grow in controlled conditions (22°C day (16h) / 18°C night (8h) cycle) in the growth
324 shelf. Once the plants were 3.5 weeks old, 2 leaves were collected and used for colony-forming unit
325 (CFU) counting. The leaves were ground in sterile 1x PBS by bead beating (1400 rpm for 30s) and a
326 dilution series was prepared. This was plated onto R2 agar and incubated for 48 h before CFU counting.
327 Based on a bacterial load higher than the wild-type, siliques were harvested from individual plants (n=1
328 in the M2 generation, Method Fig.1). Bacterial loads were further tested by CFU counting in the
329 subsequent generations and for this study, one of the mutants with the highest bacterial load and a
330 unique phenotype (CLLF) was used for further experiments. All described experiments were carried
331 out with at least M4 generation seeds.

332 *Plant growth conditions*

333 For microbiome analysis of plants colonized from the soil, seeds of the *A. thaliana* NG2 wildtype
334 (hereafter NG2) and the mutant genotype CLLF were surface sterilized by washing for 2 min in 2%
335 bleach followed by 30s in 70% ethanol and 2 sterile water rinses. They were sown onto commercial
336 soil supplemented with garden soil inoculum (See method section 1) after vernalization in 0.1% agarose
337 at 4°C for 5 days. Later, a plastic wrap was used to cover individual pots, leaving a small hole in the
338 middle to allow the seedling to germinate. This acted as a barrier between the leaves and soil, preventing
339 detection of any soil microbes on leaves due to increased soil contact in CLLF (Barrier Experiment).
340 Plants were then allowed to grow at 22°C day (16h) / 18°C night (8h) for 3 weeks in a plant climate
341 chamber (PolyKlima, Freising, Germany) before leaf harvest. Each sample represents 4 leaves from a
342 single plant. No plastic barrier was used for replicate experiments in which leaves were used either for
343 total microbiome or phytohormone analysis. For phytohormone analysis, commercial soil without
344 garden soil inoculum was used. For gnotobiotic growth, surface sterilized and vernalized seeds were
345 sowed into Linsmaier and Skoog media (4.3g/L LS salt mix (Linsmaier & Skoog (1964)), 1% sucrose,
346 0.5% MES, 0.3% phytigel) solidified in sterile 24 well plates.

347 *Plant DNA extraction*

348 We used a high throughput DNA extraction method to isolate DNA from leaves. 2-6 leaves were taken
349 for DNA extraction depending on the weight and after washing away dust and debris with autoclaved
350 Milli-Q water, were frozen at -80°C. Later, frozen samples were ground in a bead beater at 1400rpm,
351 for 30s to 60s to make a fine homogenate using 3mm metal and 0.25-0.5 mm glass beads. DNA was
352 extracted in CTAB (2% (w/v) Cetyltrimethylammoniumbromid, 100mM Tris with pH 8.0, 20mM EDTA
353 with pH 8, 1,4M NaCl, 1% (w/v) Polyvinylpyrrolidone) buffer and then purified from the lysate using
354 Phenol:Chloroform:Isoamyl alcohol (25:24:1) and precipitated using 0.7 volume 2-propanol.
355 Precipitated DNA was then dissolved in 10mM-Tris buffer for the barrier experiment or nuclease-free
356 water for the remaining microbiome analysis.

357 *16S rRNA gene amplicon sequencing*

358 For amplicon library preparation, we used a modified version of the host-associated microbe PCR
359 (hamPCR) protocol (17). Kapa HiFi enzyme (Roche; 07958846001) was used for all PCR reactions.
360 Zymomix, nuclease-free water, and CTAB extraction buffer were used as internal controls to evaluate
361 contamination and sequencing depth. In the first tagging step, we used universal primers targeting the
362 V3-V4 region of 16S rDNA modified with a 5' overhang. In addition to that, we used primers targeting
363 host-specific single copy gene (GIGANTEA or GI gene) and blocking oligos to limit the amplification
364 of chloroplast 16S rDNA (34). Each 10 μ L 1st PCR mix contained 1x Kapa Buffer, 0.3 mM Kapa
365 dNTPs, 0.08 μ M of each of the forward and reverse 16S rDNA and GI primers, 0.25 μ M of each of the
366 blocking oligos, 0.2 μ L Kapa HiFi DNA polymerase, and 50 to 100 ng template genomic DNA.
367 Thermocycling steps included initial denaturation at 95°C for 3min, denaturation at 98°C for 20s, two-
368 step annealing at 58°C for 30s and 55°C for 1min, extension at 72°C for 1min (cycle repeated 5x), and
369 final extension at 72°C for 2min. An enzymatic cleanup was done to remove primer dimers and
370 inactivate nucleotides by directly adding 0.5 μ L of Antarctic phosphatase and Exonuclease 1 (New
371 England Biolabs, Inc; M0293L, M0289L) and 1.22 μ L Antarctic phosphatase buffer (1x final
372 concentration) to the 1st PCR mix. It was then incubated at 37°C for 30 minutes followed by 80°C for
373 15 minutes to inactivate the enzyme activity. Next, in a second PCR barcoded primers targeted the 5'
374 overhangs to amplify 1st PCR products. The 20 μ L 2nd PCR mix contained 1x Kapa Buffer, 0.375 mM
375 Kapa dNTPs, 0.3 μ M of each forward and reverse primer, 0.5 μ L Kapa HiFi DNA polymerase, and 5 μ L
376 1st PCR product. The PCR program included initial denaturation 95°C for 3min, denaturation at 98°C
377 for 20s, annealing at 60°C for 1min, extension at 72°C for 1min (repeated 35x), and final extension at
378 72°C for 2min. The barcoded PCR products from the second PCR were cleaned by magnetic separation
379 using Sera mag beads. Later, we estimated the concentration of each sample by measuring fluorescence
380 using PicoGreen (Quant-iT™ PicoGreen™). After adjusting the concentration, all samples were pooled
381 into one single library and concentrated using sera mag beads. The concentrated library was then loaded
382 into a 2% agarose gel and stained with Roti gel stain. The separated GI and 16S rDNA bands were cut
383 out of the gel and DNA was eluted from each of the gel pieces using the GeneJET gel extraction kit
384 (Thermo Scientific™; K0691). After measuring the concentration of gel-eluted DNA, a final library
385 was prepared with an adjusted concentration of 95% 16S rDNA and 5% GI. We quantified the final
386 library with a Qubit (Thermo Fisher Scientific, Inc). Then the library was denatured and loaded onto a
387 MiSeq lane spiked with 10% PhiX genomic DNA to ensure sequence diversity. Using conventional
388 Illumina sequencing primers, 600 cycles of Illumina sequencing were carried out to obtain 300 bp
389 sequences in both the forward and reverse directions.

390 *Amplicon sequencing data processing*

391 For all datasets, adapter sequences were first removed from reads using Cutadapt 3.5 and reads were
392 split into samples according to barcodes using a custom script. Quality filtering and clustering the data
393 into amplicon sequencing variants (ASVs) were performed with the dada2 (version 1.18.0) algorithm,

394 using only forward reads because of its higher quality. Taxonomy was assigned to the ASVs using
395 dada2 with the Silva 16S rDNA database (version 138.1) supplemented with the *A. thaliana* GI gene
396 sequence. We examined positive and negative controls from all data sets. Positive control (Zymomix)
397 had an expected distribution of taxa and negative controls had very few reads (<60 reads) suggesting
398 minimal contaminations, so these were not processed further. R packages Phyloseq (version 1.34.0),
399 VEGAN (version 2.5-7), and DEseq2 (version 1.44.0), were used for downstream analysis. Host-
400 derived reads were removed from the ASV tables by removing family "Mitochondria", order
401 "Chloroplast" and Genus "Arabidopsis GI". In addition, all samples were normalized to GI reads before
402 analysis so that diversity patterns reflect the true abundances of leaf bacteria. Plant GI reads were also
403 used to normalize the total number of bacterial reads to get an estimate of the relative bacterial loads of
404 each sample. Other packages such as ggplot2, reshape2, and ggpubr were used for statistical analysis
405 and plotting data. Scripts for generating the main figures from the ASV tables and metadata will be
406 made publicly available on Figshare prior to publication.

407 *Assessing plant survival rate in a garden experiment*

408 To compare survival rates of CLLF and NG2, we germinated seeds in a mix of 1:4 garden soil to
409 commercial soil (as described above) under laboratory conditions. Plants were sown into 7 replicate
410 trays, each divided into two halves, one for each genotype. Plants were thinned to 30 seedlings of each
411 genotype per tray, which was considered as one replicate. The trays with seedlings were moved to the
412 garden 7 days after germination (in Nov 2022), and the number of plants surviving in each tray was
413 counted every week until plants started flowering (in March 2023).

414 *Phytohormone analysis*

415 For the phytohormone extraction, we used a high-throughput method previously published by Schäfer
416 et al. (2016). We collected 100mg of leaves from 3-week-old lab-grown plants in a pre-weighed 2mL
417 screw-cap tube with two metal beads each. Then we fast-froze the samples in liquid nitrogen and stored
418 at -80°C until further processing. The frozen samples were ground into a fine powder using a tissue
419 lyser (MiniG 1600, SPEX Sample Prep). For the extraction, samples were homogenized in 15:4:1
420 (v/v/v) methanol: H₂O: formic acid extraction buffer containing isotope-labeled phytohormone
421 standards, centrifuged at high speed, and the supernatant was collected. The supernatant was then
422 passed through a reversed-phase solid-phase extraction (SPE) column (HR-X, Machery-Nagel,
423 738530.025M). Methanol from the flow-through was then allowed to evaporate and the remaining
424 samples were reconstituted in 1N formic acid. Reconstituted samples were then passed through a mixed-
425 mode cation exchange SPE column (HR-XC, Machery-Nagel, 738540.025M), and the flow through
426 was discarded. The column was washed once with 1N formic acid and eluted using an 80% aqueous
427 methanol containing 0.2N formic acid. This eluted fraction contained abscisic acid (ABA), salicylic
428 acid (SA), and jasmonates (JAs), which were analyzed by LC-MS/MS on a triple-quadrupole mass
429 spectrometer (EVO-Q Elite, Bruker) using the chromatog. The chromatographic condition and

430 multiple-reaction-monitoring details for the compound detection are described in detail by Schäfer et
431 al. (35).

432 *Pathogen infection assays*

433 For the bacterial pathogen infection assay, CLLF and NG2-Wt were grown in gnotobiotic conditions in
434 LS media in square petri dishes. *Pseudomonas syringae pv syringae* DC3000 (Pst DC3000) was grown
435 in LB agar supplemented with rifampicillin for 48 h at 30°C. Colonies were then collected using a loop
436 and resuspended in 10 mM MgCl₂. OD was measured using a UV spectrometer and adjusted to 0.02
437 OD. 0.02 % Silwet L-77 was freshly added to the bacterial suspension just before flood inoculation.
438 For flood inoculation, 40mL bacterial culture was poured into the petri dishes with plants. Plants
439 inoculated with 40mL of 10 mM MgCl₂ plus 0.02 % Silwet L-77 were taken as controls. Disease
440 symptoms were measured after 24h.

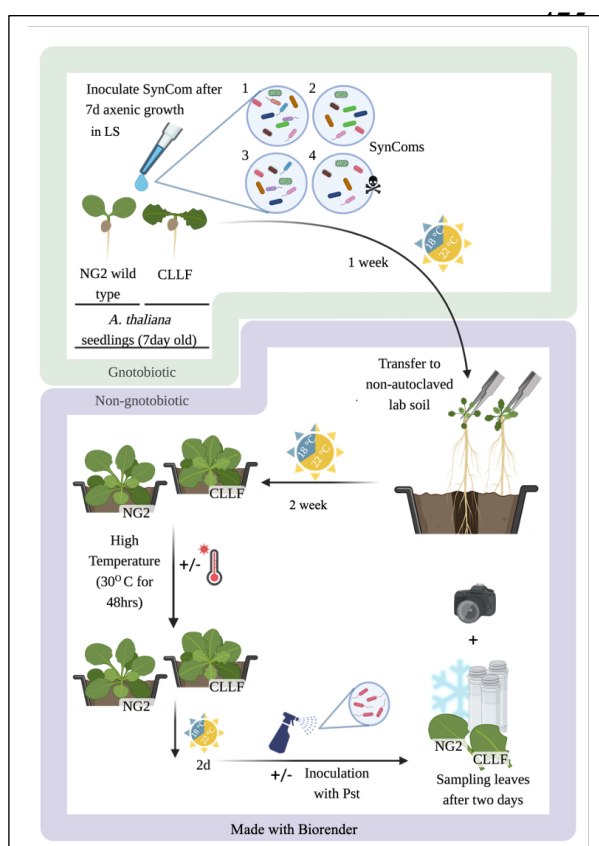
441 For the fungal infection assay, plants grown in the semi-gnotobiotic (2-week-old seedlings grown in LS
442 media transplanted into commercial soil) system. *Sclerotinia sclerotiorum* (Ssc) was grown in Potato-
443 Dextrose agar (PDA) plates from a subculture for 4-6 days. We collected agar discs from the actively
444 growing region of Ssc plates and used this to inoculate liquid PDB (Potato-Dextrose Broth). Liquid
445 culture was then allowed to grow overnight at room temperature with shaking. We harvested the
446 mycelia the next day after passing it through an autoclaved nylon membrane. After washing them with
447 autoclaved milliQ water, they were resuspended in fresh PDB. This was then macerated to get small
448 hyphal fragments using a sterile macerator. Hyphal fragments were adjusted to 2x10⁵ fragments/ml.
449 5µL of this hyphae suspension was used to inoculate leaves of 4-week-old plants. The leaf midrib was
450 avoided for easy measurement of the lesion and lesion size was measured at both 18 hours post-
451 inoculation (hpi) and 40hpi.

452 *Synthetic community preparation*

453 We used bacterial strains that were previously isolated from CLLF or NG2 leaves for preparing the
454 Synthetic Communities (SynComs) (Supplementary Table 1A). All strains were grown on R2 agar
455 plates. Depending on each strain's growth rate, it took 1 to 5 days to grow all strains. The bacteria were
456 then scraped off the plates and resuspended in 1x phosphate buffer saline (PBS). Optical density (OD)
457 was measured using a 1:10 dilution of each bacterial suspension in a plate reader. Since we observed
458 huge variation in the number of CFUs per OD of different bacteria, we decided to consider CFUs for
459 preparing SynComs. Therefore, an OD to CFU relationship of each bacterium was measured and this
460 was used to combine the bacterial suspensions into a single inoculum so that all strains would have
461 approximately same number of CFUs (~30 CFU per strain). A total of 45 strains belonging to diverse
462 plant-associated bacterial phyla constituted the SynCom1. The SynCom2 lacked strains belonging to
463 Comamonadaceae and Oxalobacteriaceae (Betaproteobacteria). SynCom3 lacked strains belonging to
464 Bacteroides and SynCom4 lacked Betaproteobacteria and Bacteroides. For each missing strain in

465 SynComs 2-4, we added the same amount of 1x PBS buffer to the SynCom stocks. In addition, aliquots
466 of all four SynComs were mixed with an equal amount of 40% glycerol for future analysis. To check
467 the SynCom compositions, 12 μ L from the glycerol stocks were later inoculated onto R2 agar plates and
468 grown for 5 days at 28°C. All cells were harvested from R2 plates by suspending into 1x PBS, and later,
469 all samples were centrifuged at 5000rpm in a table-top centrifuge and the pellet was resuspended in
470 CD1 solution of DNAeasy plant pro kit (Qiagen; 0142924730) along with 0.25-0.5 mm glass beads.
471 It was then bead-beated at 1400rpm for 30s. DNA was extracted using the kit following the suggested
472 protocol. The communities were analyzed using the 16S rRNA gene amplicon sequencing
473 pipeline as described above.

474 *Semi-gnotobiotic plant growth conditions and stress treatments*



Method Fig.2. Workflow showing SynCom experiment in a semi-gnotobiotic system. Gnotobiotic phase; Sterilized seeds of CLLF and NG2 plants were germinated in sterile LS media. 7-day old seedlings were inoculated with 5 μ L SynCom or 1X PBS. Plants were allowed to grow in LS media with or without the SynComs for 1 week at 22h day/8h night cycles. **Non-gnotobiotic phase;** 2-week-old pre-colonized plants are moved to commercial soil. After two weeks of growth (22h day/8h night cycles), half the of plants were challenged with temperature stress at 30°C for 48 h, followed by 2 days of recovery under normal condition. Later half of plants from each treatment was challenged with PstDC3000. After 2 days, leaves were sampled for microbiome or RNAseq analysis.

We noted that in fully gnotobiotic, enclosed growth systems, plants tended to become stressed by humidity. Therefore, we developed a semi-gnotobiotic system in which plants are pre-colonized by a defined community in a gnotobiotic environment and then moved to a standard, non-sterile laboratory soil and grown in trays. When we tested the semi-gnotobiotic system with a fluorescently labeled isolate of *Stenotrophomonas* sp., leaf microbiomes were dominated by *Stenotrophomonas* even after several weeks in the soil, suggesting that this is an effective inoculation strategy (36). For this study, surface-sterilized and vernalized seeds of CLLF and NG2 were sown into LS media. 7-day-old seedlings were inoculated with 5 μ L inoculum of one of the four SynComs or 1x PBS buffer. This was enough inoculum to wet the leaves and roots. There were 48 replicates per genotype and SynCom. The plants were grown for 1 week in LS before being transplanted into commercial soil at 22°C day-16h/18°C night- 8h cycles. After 2 weeks of normal growth in soil, 16 plants from each genotype inoculated with one of the 4 SynCom or 1x PBS were given heat stress by moving into a growth chamber set at 30°C day (16h)

500 and night (8h) for 48h. The remaining plants were allowed to grow at normal 22°C day-16h/18°C night-

501 8h cycles. Later the plants that underwent heat stress were moved back into normal growth conditions
502 and all plants were grown for 2 days under 22°C day-16h/18°C night condition before treating with
503 *Pseudomonas syringae* pv. *syringae* DC3000 (Pst DC3000). Half of the plants from each treatment
504 were spray-inoculated with 0.02 OD cultures of Pst DC3000 suspended in sterile milliQ water
505 supplemented with 0.02% Silwet L-77 and the remaining half with sterile milliQ water. After 48 hours
506 post-inoculation, we measured leaf function using an LI-COR 600, and 2-3 leaves from at least 6 plants
507 were sampled for microbiome analysis from all the different treatments. 2-3 leaves from SynCom 1, 4,
508 and negative controls with and without heat stress were sampled for RNAseq analysis (Method Fig. 2).

509 *RNA sequencing and data processing*

510 All samples for RNAseq were fast-frozen using liquid nitrogen and stored at -80°C. The samples were
511 then ground to a fine powder in a bead beater using 2 metal beads. Finely ground samples were used
512 for RNA isolation using the RNeasy Plant Mini Kit (Qiagen, ID: 74904). Total RNA was sent to
513 Eurofins genomics for rRNA depletion, cDNA synthesis, library preparation and sequencing. Raw data
514 received from Eurofins Genomics were then used for downstream processing as follows. Raw
515 sequencing reads were assessed for quality using FastQC (version
516 0.11.9; <https://www.bioinformatics.babraham.ac.uk/projects/fastqc>). Adaptor trimming, quality
517 filtering, and read preprocessing were performed using fastp (version 0.23.2) (37). In detail, 5' and 3'
518 bases with a Phred quality score below 28 were cut and reads were removed if they had more than one
519 ambiguous base, an average quality score below 28, or a length of fewer than 15 bases. Processed reads
520 were aligned to the current *A. thaliana* genome (tair10.1) using Hisat2 (version 2.2.1) with standard
521 parameters (38). The aligned reads were sorted and indexed using SAMtools (version 1.11) (39). Read
522 counting was performed using featureCounts (version 2.0.1) (40) with the tair10.1 annotation as a
523 reference. Differential gene expression analysis was performed using DESeq2 (version 1.38.3) (41) and
524 comparisons having a false discovery rate (FDR) adjusted p-value <0.05 were deemed to be statistically
525 significant (42). Gene ontology (GO) enrichment was performed for each DE gene set using the R
526 package, clusterProfiler (version 4.10.0), and the GO category was assigned using the annotation data
527 package org.At.tair.db (version 3.18.0). The detailed scripts with step-by-step instructions were
528 uploaded to GitHub (https://github.com/Bioinformatics-Core-Facility-Jena/SE20231212_167).

529 *Growth assay with salicylic acid*

530 All strains belonging to Betaproteobacteria and Bacteroides and representative strains from the
531 remaining major taxonomic groups of the SynComs were used for growth assays. First, bacteria were
532 grown in R2 agar at 28°C for 4 days. Fresh colonies were then harvested from agar plates using a sterile
533 loop and resuspended in 1x PBS by vortexing and repeated pipetting. After measuring the optical
534 density (OD₆₀₀), the OD₆₀₀ of all samples was adjusted to 0.02. 10 µL of this pre-adjusted culture was
535 used as an inoculum for measuring growth in 190 µL of M9 minimal media (M9 salts: 33.7mM
536 Na₂HPO₄, 22mM KH₂PO₄, 8.55mM NaCl, 9.35mM NH₄Cl, and 2 mM MgSO₄*7H₂O, 0.2 mM CaCl₂, 1
537 µg/mL biotin, 1 µg/mL thiamine, and trace elements: 134 µM EDTA, 31 µM FeCl₃-6H₂O, 6.2 µM

538 ZnCl₂, 0.76 μM CuCl₂·2H₂O, 0.42 μM CoCl₂·2H₂O, 1.62 μM H₃BO₃, 0.081 μM MnCl₂·4H₂O)
539 supplemented either with 0.5mM Salicylic acid (SA), concentration adapted from S. L. Lebeis, *et al* (9),
540 11 mM Fructose plus 11 mM Sucrose (PC) or no additional carbon source (Control) for the growth
541 assay. All samples were then incubated at 28°C with shaking (220rpm) in 15-minute intervals in a plate
542 reader for 5 days. OD₆₀₀ was measured every 1.5 h.
543

544 Competing Interest Statement

545 The authors declare no competing interests.

546 Data Sharing Plan

547 Data needed to evaluate the conclusions in the paper are present in the paper and/or the Supplementary
548 Materials. Raw sequencing data is available on NCBI-SRA (16S data: PRJNA1120601, RNAseq
549 data: XXX) and processed data with code to generate the main figures will be available on Figshare
550 before final publication. The detailed scripts with step-by-step instructions for RNA-seq analysis were
551 uploaded to GitHub (https://github.com/Bioinformatics-Core-Facility-Jena/SE20231212_167).

552 Funding Information

553 Carl Zeiss Foundation via Jena School for Microbial Communication (JJ, MTA)

554 Deutsche Forschungsgemeinschaft (DFG, German Research Foundation) under Germany's
555 Excellence Strategy - EXC 2051 - Projektnummer 390713860 (JJ, MTA, MM)

556 Max Planck Society (RH)

557 The Ministry for Economics, Sciences and Digital Society of Thuringia (TMWWDG), under the
558 framework of the Landesprogramm ProDigital [DigLeben-5575/10-9]. (EB)

559

560 Deutsche Forschungsgemeinschaft (DFG, German Research Foundation) under CRC 1076
561 'AquaDiva', subproject A06. (MM)

562

563 References

- 564
- 565 1. McNew, George L., “The nature origin and evolution of parasitism” in *Plant Pathology: An*
566 *Advanced Treatise*, (Academic Press, 1960), pp. 19–69.
- 567 2. F. Entila, X. Han, A. Mine, P. Schulze-Lefert, K. Tsuda, Commensal lifestyle regulated by a
568 negative feedback loop between Arabidopsis ROS and the bacterial T2SS. *Nat. Commun.* **15**, 456
569 (2024).
- 570 3. L. Maignien, E. A. DeForce, M. E. Chafee, A. M. Eren, S. L. Simmons, Ecological Succession and
571 Stochastic Variation in the Assembly of Arabidopsis thaliana Phyllosphere Communities. *mBio* **5**
572 (2014).
- 573 4. K. M. Meyer, *et al.*, Plant neighborhood shapes diversity and reduces interspecific variation of
574 the phyllosphere microbiome. *ISME J.* **16**, 1376–1387 (2022).
- 575 5. T. Chen, *et al.*, A plant genetic network for preventing dysbiosis in the phyllosphere. *Nature* **580**,
576 653–657 (2020).
- 577 6. P. J. P. L. Teixeira, *et al.*, Specific modulation of the root immune system by a community of
578 commensal bacteria. *Proc. Natl. Acad. Sci.* **118**, e2100678118 (2021).
- 579 7. S. Pfeilmeier, *et al.*, The plant NADPH oxidase RBOHD is required for microbiota homeostasis in
580 leaves. *Nat. Microbiol.* **6**, 852–864 (2021).
- 581 8. C. J. Harbort, *et al.*, Root-Secreted Coumarins and the Microbiota Interact to Improve Iron
582 Nutrition in Arabidopsis. *Cell Host Microbe* **28**, 825-837.e6 (2020).
- 583 9. S. L. Lebeis, *et al.*, Salicylic acid modulates colonization of the root microbiome by specific
584 bacterial taxa. *Science* **349**, 860–864 (2015).
- 585 10. K. Unger, *et al.*, Beyond defense: Glucosinolate structural diversity shapes recruitment of a
586 metabolic network of leaf-associated bacteria. [Preprint] (2023). Available at:
587 <http://biorxiv.org/lookup/doi/10.1101/2023.12.04.567830> [Accessed 13 May 2024].
- 588 11. B. Huot, *et al.*, Dual impact of elevated temperature on plant defence and bacterial virulence in
589 Arabidopsis. *Nat. Commun.* **8**, 1808 (2017).
- 590 12. J. Qiu, *et al.*, Warm temperature compromises JA-regulated basal resistance to enhance
591 Magnaporthe oryzae infection in rice. *Mol. Plant* **15**, 723–739 (2022).
- 592 13. H.-G. Mang, *et al.*, Abscisic Acid Deficiency Antagonizes High-Temperature Inhibition of Disease
593 Resistance through Enhancing Nuclear Accumulation of Resistance Proteins SNC1 and RPS4 in
594 Arabidopsis. *Plant Cell* **24**, 1271–1284 (2012).
- 595 14. A. Issa, *et al.*, Impacts of Paraburkholderia phytofirmans Strain PsJN on Tomato (Lycopersicon
596 esculentum L.) Under High Temperature. *Front. Plant Sci.* **9**, 1397 (2018).
- 597 15. R. J. Rodriguez, *et al.*, Stress tolerance in plants via habitat-adapted symbiosis. *ISME J.* **2**, 404–
598 416 (2008).
- 599 16. Mayer, Teresa, “Whose microbiome is it? Adaptive interactions of keystone species in plant
600 microbiomes.” Friedrich Schiller University of Jena, Jena, Germany. (2022).

- 601 17. D. S. Lundberg, *et al.*, Host-associated microbe PCR (hamPCR) enables convenient measurement
602 of both microbial load and community composition. *eLife* **10**, e66186 (2021).
- 603 18. S. A. Vincent, A. Ebertz, P. D. Spanu, P. F. Devlin, Salicylic Acid-Mediated Disturbance Increases
604 Bacterial Diversity in the Phyllosphere but Is Overcome by a Dominant Core Community. *Front.*
605 *Microbiol.* **13**, 809940 (2022).
- 606 19. L.-J. Wang, *et al.*, Salicylic acid alleviates decreases in photosynthesis under heat stress and
607 accelerates recovery in grapevine leaves. *BMC Plant Biol.* **10**, 34 (2010).
- 608 20. T. L. Karasov, *et al.*, The relationship between microbial population size and disease in the
609 *Arabidopsis thaliana* phyllosphere. [Preprint] (2019). Available at:
610 <http://biorxiv.org/lookup/doi/10.1101/828814> [Accessed 13 May 2024].
- 611 21. K. Ogata, M. Ohsugi, M. Tomita, T. Tochikura, The Production of α -Ketoglutaric Acid from
612 Salicylic Acid by *Pseudomonas* sp.†. *Agric. Biol. Chem.* **34**, 364–369 (1970).
- 613 22. G.-H. Lim, *et al.*, Plasmodesmata Localizing Proteins Regulate Transport and Signaling during
614 Systemic Acquired Immunity in Plants. *Cell Host Microbe* **19**, 541–549 (2016).
- 615 23. W. Liu, S.-W. Park, 12-oxo-Phytodienoic Acid: A Fuse and/or Switch of Plant Growth and Defense
616 Responses? *Front. Plant Sci.* **12**, 724079 (2021).
- 617 24. I. Monte, *et al.*, An Ancient CO11-Independent Function for Reactive Electrophilic Oxylipins in
618 Thermotolerance. *Curr. Biol.* **30**, 962-971.e3 (2020).
- 619 25. M. Antunez-Lamas, *et al.*, Bacterial chemoattraction towards jasmonate plays a role in the entry
620 of *Dickeya dadantii* through wounded tissues. *Mol. Microbiol.* **74**, 662–671 (2009).
- 621 26. O. S. Kulkarni, *et al.*, Volatile methyl jasmonate from roots triggers host-beneficial soil
622 microbiome biofilms. *Nat. Chem. Biol.* **20**, 473–483 (2024).
- 623 27. C. S. Liou, *et al.*, A Metabolic Pathway for Activation of Dietary Glucosinolates by a Human Gut
624 Symbiont. *Cell* **180**, 717-728.e19 (2020).
- 625 28. H.-W. Jeon, *et al.*, Contrasting and conserved roles of NPR pathways in diverged land plant
626 lineages. [Preprint] (2022). Available at:
627 <http://biorxiv.org/lookup/doi/10.1101/2022.07.19.500630> [Accessed 13 May 2024].
- 628 29. Y. Liu, *et al.*, Diverse Roles of the Salicylic Acid Receptors NPR1 and NPR3/NPR4 in Plant
629 Immunity. *Plant Cell* **32**, 4002–4016 (2020).
- 630 30. J. H. Kim, *et al.*, Increasing the resilience of plant immunity to a warming climate. *Nature* **607**,
631 339–344 (2022).
- 632 31. M. R. Wagner, *et al.*, Host genotype and age shape the leaf and root microbiomes of a wild
633 perennial plant. *Nat Commun* **7**, 12151 (2016).
- 634 32. B. N. Archibald, V. Zhong, J. A. N. Brophy, Policy makers, genetic engineers, and an engaged
635 public can work together to create climate-resilient plants. *PLOS Biol.* **21**, e3002208 (2023).
- 636 33. D. Weigel, J. Glazebrook, EMS Mutagenesis of *Arabidopsis* Seed. *Cold Spring Harb. Protoc.* **2006**,
637 pdb.prot4621 (2006).

- 638 34. T. Mayer, *et al.*, Obtaining deeper insights into microbiome diversity using a simple method to
639 block host and nontargets in amplicon sequencing. *Mol. Ecol. Resour.* **21**, 1952–1965 (2021).
- 640 35. M. Schäfer, C. Brütting, I. T. Baldwin, M. Kallenbach, High-throughput quantification of more
641 than 100 primary- and secondary-metabolites, and phytohormones by a single solid-phase
642 extraction based sample preparation with analysis by UHPLC–HESI–MS/MS. *Plant Methods* **12**,
643 30 (2016).
- 644 36. Teutloff, Erik, “Balance in plant bacterial recruitment affects resilience to fungal invasion of the
645 phyllosphere,” Friedrich Schiller University of Jena, Jena, Germany. (2023).
- 646 37. S. Chen, Y. Zhou, Y. Chen, J. Gu, fastp: an ultra-fast all-in-one FASTQ preprocessor.
647 *Bioinformatics* **34**, i884–i890 (2018).
- 648 38. D. Kim, J. M. Paggi, C. Park, C. Bennett, S. L. Salzberg, Graph-based genome alignment and
649 genotyping with HISAT2 and HISAT-genotype. *Nat. Biotechnol.* **37**, 907–915 (2019).
- 650 39. H. Li, *et al.*, The Sequence Alignment/Map format and SAMtools. *Bioinformatics* **25**, 2078–2079
651 (2009).
- 652 40. Y. Liao, G. K. Smyth, W. Shi, featureCounts: an efficient general purpose program for assigning
653 sequence reads to genomic features. *Bioinformatics* **30**, 923–930 (2014).
- 654 41. M. I. Love, W. Huber, S. Anders, Moderated estimation of fold change and dispersion for RNA-
655 seq data with DESeq2. *Genome Biol.* **15**, 550 (2014).
- 656 42. Y. Benjamini, Y. Hochberg, Controlling the False Discovery Rate: A Practical and Powerful
657 Approach to Multiple Testing. *J. R. Stat. Soc. Ser. B Stat. Methodol.* **57**, 289–300 (1995).
- 658